HEAT TRANSFER CAPACITY OF A HEAT EXCHANGER MODULE FOR SEASONAL HEAT STORAGE

Jianhua Fan, Simon Furbo, Ziqian Chen, Elsa Andersen and Bengt Perers

Department of Civil Engineering, Technical University of Denmark, Kgs. Lyngby, Denmark

1. Introduction

Theoretical investigations have shown that a solar heating system with a collector area of 36 m² can fully cover the yearly heat demand of a low energy house in Denmark if the solar heating system is based on a 6000 l seasonal heat storage with sodium acetate trihydrate (SAT) supercooling in a stable way. The heat storage is divided into a number of separate modules. As shown in Fig. 1, a sandwich heat storage test module has been built with the phase change material (PCM) storage box in between two plate heat exchangers. The plate heat exchanger at the top of the PCM storage box is used for discharge of the module while the plate heat exchanger at the bottom is used for charge of the module. The test module has a length of approx. 2060 mm and a width of approx. 1330 mm. The height of the plate heat exchangers is 13 mm. Fluid flow in the plate heat exchangers are regulated by a number of parallel baffles.

Thermal experiments have been carried out to investigate the heat exchange capacity rates from and to the PCM module. Charge of the PCM module is investigated with solid phase SAT and with supercooled liquid phase SAT as initial condition. Discharge of the PCM module with and without the presence of crystallization is studied. Fluid flow and heat transfer in the test module are theoretically investigated by Computational Fluid Dynamics (CFD) calculations. The heat transfer rates between the PCM box and the heating fluid/cooling fluid in the plate heat exchangers are determined. The CFD calculated temperatures are compared to measured temperatures. Based on the studies, recommendations on how best to transfer heat to and from the seasonal heat storage module will be given.

2. The experimental setup

Theoretical calculations by Schultz and Furbo (2007) have shown that the heat exchange capacity rates both for charge and discharge of a seasonal heat storage module for solar heating systems fully covering the yearly heat demand of low energy buildings must be around 500 W/K. The tested heat storage module based on stable supercooling of sodium acetate trihydrate (SAT) has an approximate volume of 234 l, corresponding to about half the volume of a suitable heat storage module for a real seasonal heat storage. It is therefore estimated that the heat exchange capacity rate for the investigated heat storage module must be around 250 W/K.

A flat laboratory heat storage module described by Furbo et al. (2010) is investigated experimentally. Figure 1 shows a photo of the heat storage module. The module is filled with 305 kg salt water mixture consisting of 58% (weight%) sodium acetate and 42% (weight%) water. The volume of the salt water mixture is about 234 l. The salt water mixture is used, since it supercools in a stable way. Investigations by Furbo (1978) have shown that a salt water mixture of 58% $NaCH_3COO$ and 42% water can be used in tanks made from steel without a risk of corrosion. The module material is therefore steel and the wall thickness is 2 mm. The test module has a length of approx. 2060 mm and a width of approx. 1330 mm. The height of the plate heat exchangers is 13 mm.

The aim of the investigations is to determine the heat exchange capacity rate of the PCM module during charge and discharge. A plate heat exchanger is mounted at the top of the PCM storage module for discharge of the module while a plate heat exchanger is mounted at the bottom for charge of the module. In order to avoid dead zones and uneven flow distribution, a number of parallel silicon pipe baffles are installed in the flat plate heat exchangers to regulate the fluid flow. During charge of the module, hot water flows into the bottom plate heat exchanger and transfers heat to the PCM module through the bottom surface of the module, whereas during discharge of the module cold water flows into the upper plate heat exchanger and absorbs

heat through the upper surface of the PCM module. The sandwich like heat storage module is insulated with mineral wool or insulation foam on all external surfaces of the module.

The water volume flow rate during charge and discharge of the module is regulated by a circulation pump and a valve. The circulating flow rate, in the range of 3.0-8.5 l/min, is measured using a Brunata type HGQ1-R0 flow meter. The inlet and outlet water temperatures of the heat exchangers are measured by copper-constantan thermo couples (type TT). The temperature of the PCM store can not be measured directly since insertion of temperature sensors into the store prevents stable supercooling of SAT and must therefore be avoided. The temperature of the PCM store can be estimated by measurement of temperatures on the surfaces of the store. The surface temperatures of the PCM store are measured by 12 equally spaced thermocouples (type TT) with 6 sensors attached to the upper surface and 6 sensors attached to the bottom surface of the store. The data collection and control program IMPVIEW is used to log the fluid flow rate, the inlet and outlet temperatures of the heat exchanger, the surface temperatures of the PCM store and the ambient temperature during the test period. The accuracy of the flow rate measurement is ± 1 % while the accuracy of the type TT thermocouples is ± 0.5 K.

Fig. 1: Photo of the PCM heat storage test module with plate heat exchangers at the top and the bottom.

3. The computational fluid dynamics model

Computation fluid dynamics calculations are carried out to theoretically investigate the fluid flow and heat transfer in the heat storage module during charge and discharge. Simplified heat storage models (charge model and discharge model) are built using the commercial CFD code Ansys (Fluent) 13 (2010). The charge model includes the PCM box and the flat plate heat exchanger mounted at the bottom surface of the PCM box while the heat exchanger at the top of the PCM box is an inactive component and thus not considered, see Fig. 2. During charging, the hot water enters into the plate heat exchanger through an inlet opening located in one corner of the exchanger and leaves the heat exchanger through an outlet opening in the opposite corner. Water flow in the heat exchanger is regulated by 18 equally spaced guiding baffles, resulting in a serpentine flow pattern. The height of the water passage is 13 mm. The heat loss coefficient of the PCM storage module is determined by measurements and used as an input to the CFD models. The measured mean ambient air temperature during the experiment is used as free stream temperature of the module surfaces in the CFD models. In this way, the CFD model takes into account the heat loss from the storage module.

The discharge model includes the PCM box and the flat plate heat exchanger mounted at the upper surface of the PCM box while the heat exchanger at the bottom of the PCM box is excluded.

Mesh of the PCM module during charge is shown as an example in Fig. 3. Fig. 3(A) shows mesh at the horizontal plan of the module. The serpentine flow passage created by the guiding baffles is meshed with high quality hexahedral elements with an interval size of 0.01 mm. Mesh at a vertical cut plane in one corner of the module is shown as View A in Fig. 3(B). The model includes the PCM box at the top and the heat

exchanger at the bottom. A denser mesh is applied to the heat exchanger where a larger temperature/velocity gradient is expected. The mesh close to the walls is refined in order to capture the large temperature/velocity gradients in the near wall regions. In between the PCM box and the heat exchanger, there is a steel wall meshed with one node. Both vertical and horizontal conductive heat transfer in the solid steel wall are considered. The model has a mesh with approx. 462000 cells in total.

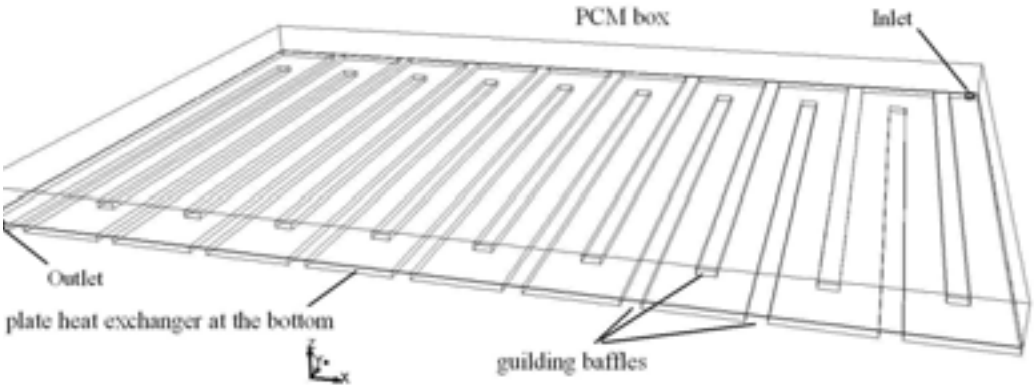

Fig. 2: CFD model of the PCM module during charge.

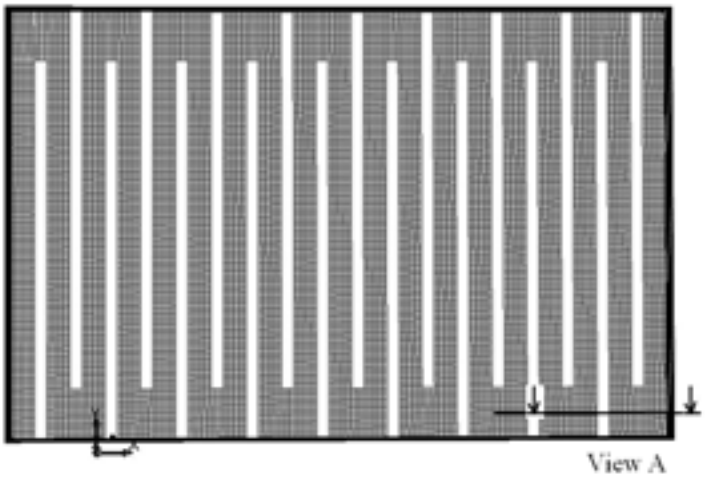

(A) Mesh at the horizontal plan of the module

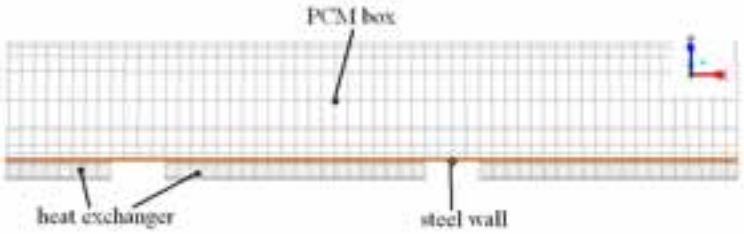

(B) Mesh of the module View A

Fig. 3: Mesh of the PCM module during charging.

During charge and discharge of the module, phase transitions of SAT between solid and liquid phase will have a significant influence on the heat transfer in the PCM module. Due to the complexity of a multi-phase CFD model, it is however desirable to start the investigation with simplified single liquid phase and single solid phase models. A CFD model of single phase liquid PCM and a model of single phase solid PCM are built. Properties of liquid mixture of 42% (weight) water and 58% (weight) NaCH3COO and their dependences on temperature are shown as follows [Yoon etc. 2000, Araki etc. 1995]:

Density, [kg/m^3] $$\rho = 1579 - 0.780 * T \quad (1)$$

Specific heat, [J/(Kg.K)] $C_p = 1594 + 4.33 * T$ (2)

Thermal conductivity, [W/(mK)] $\lambda = -2.72 + 0.0214 * T - 3.63 \times 10^{-5} * T^2$ (3)

Dynamic viscosity, [kg/(ms)] $\mu = 0.110 - 2.67 \times 10^{-4} * T$ (4)

where T is fluid temperature, [K].

Properties of solid PCM and their dependences on temperature are shown as follows [Araki etc. 1995]:

Density, [kg/m^3] Constant = 1530

Specific heat, [J/(Kg.K)] $C_p = 1017 + 3.50 * T$ (5)

Thermal conductivity, [W/(mK)] Constant = 0.6

where T is fluid temperature, [K].

Water is used to charge and discharge the PCM module. Properties of water and their dependences on temperature are shown as follows:

Density, [kg/m^3] $\rho = 863 + 1.21 * \mathrm{T} - 0.00257 * \mathrm{T}^2$ (6)

Dynamic viscosity, [kg/(ms)] $\mu = 0.0007 * (\frac{T}{315})^{-5.5}$ (7)

Thermal conductivity, [W/(mK)] $\lambda = 0.375 + 8.84 \times 10^{-4} * T$ (8)

where T is fluid temperature, [K].

The steel wall has a thermal conductivity of 60 W/K/m and a density of 7850 kg/m^3.

Investigation is carried out to determine the influence of time step size on predicted heat exchange capacity rate between the PCM store and water. Fig. 4 show CFD predicted heat exchange capacity rates of a discharge test with a volume flow rate of 5.4 l/min and a constant inlet temperature of 13.9ºC. The test starts with an initially uniform temperature of 75ºC. It is shown that the increase of the time step size from 3 s to 30 s does not influence the predicated heat exchange capacity rate. Further increase of the time step size to 60 s shows a slight variation of predicted heat exchange capacity rate in the first half hour of the test. Increase of the time step size to 120 s shows a remarkable change of predicted heat exchange capacity rate in the first hour of the test. It can be concluded that the best time step size is 30 s.

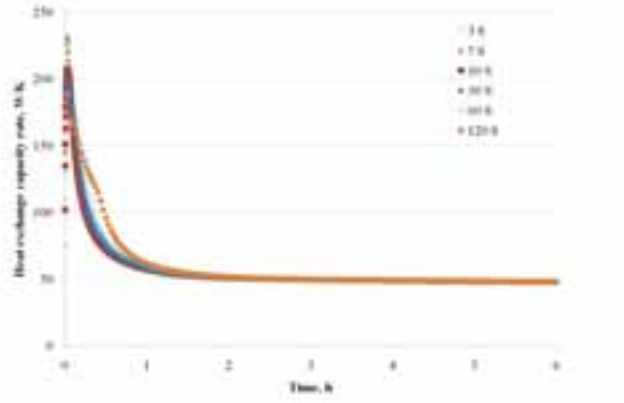

Fig. 4: The influence of time step size on heat exchange capacity rate during a discharge.

Since water flow in the plate heat exchanger mostly falls in the transitional or turbulent region, RNG modified k-ε turbulent model is used in the CFD calculations. Fluid flow in the PCM box is calculated with a laminar model. Transient CFD calculations are performed with an initially standstill module (all fluid velocities are zero) and a uniform temperature. The PRESTO and second order upwind method are used for the discretization of the pressure and the momentum equations respectively. The SIMPLE algorithm is used to treat the pressure-velocity coupling. The calculation is considered convergent if the scaled residual for the continuity equation, the momentum equations and the energy equation are less than 1.0×10^{-4}, 1.0×10^{-4} and 1.0×10^{-7} respectively. One calculation takes approximately 10-48 hours for a computer with 2×3 GHz CPU

frequency and 4G memory.

4. Result and discussion

In order to determine the heat exchange capacity rate from and to the PCM module, charge and discharge test of the PCM module have been carried out with different volume flow rates. Power of heat exchange and heat exchange capacity rate between water and the PCM store are determined. The power of heat exchange between the charging/discharging flow and the PCM store, P, is determined by equation (9).

$$P = \rho V C_p abs(T_f - T_r) \quad (9)$$

Heat exchange capacity rate, H, is determined by equation (10).

$$H = -V C_p \rho ln\left(1 - \frac{T_f - T_r}{T_f - T_s}\right) \quad (10)$$

H is heat exchange capacity rate in W/K. V is the volume flow rate of the charging/discharging flow in m^3/s. C_p is specific heat of the fluid in J/kg/K. ρ is density of the fluid in kg/m^3. T_f, T_r and T_s is respectively the inlet temperature, outlet temperature of the charging/discharging flow and temperature of the PCM store. Temperature of the PCM store, T_s, cannot be measured directly in the experiment due to the fact that insertion of temperature sensors in the PCM store prevents stable supercooling of the PCM and therefore must be avoided. Temperature of the PCM store is measured indirectly by temperature sensors attached to the upper and the bottom surface of the module. During charging of the PCM store, temperature of the PCM store can be estimated by an average of all surface temperatures or by an average of upper surface temperatures. Due to the relatively low thermal conductivity of the solid phase and liquid phase sodium acetate tri-hydrate, it is expected that heat transfer within the PCM material contributes to most of the thermal resistance of the module while the heat transfer between the steel wall and the circulating water has a much smaller thermal resistance. Therefore the bottom surface temperature of the steel wall is almost the same as the mean water temperature during the test. Before the PCM material is fully melted, the heat will be used to melt the PCM material, resulting in a stepwise temperature change in the store. Average of all surfaces temperatures of the module, T_{mean}, therefore overestimates temperature of the module, whereas average of the upper surface temperatures, T_{upper}, underestimates temperature of the PCM module.

4.1 Charge of solid phase PCM

Charge of the PCM module has been investigated at a volume flow rate of 3.4 l/min, 4.9 l /min and 6.3 l/min respectively. The charge test starts with a uniform module temperature of 17-21ºC and with a constant water inlet temperature of 77-80ºC. Fig. 5-6 show the charging power versus temperature of the PCM store at charging volume flow rates of 3.4 l/min and 6.3 l/min respectively. At the start of the charging process the power reaches up to 11000 W followed by a rapid decrease to approx. 4000 W. The extremely large charging power can be explained by the replacement of cold water by hot water in the heat exchanger in the start of the test.

It can be seen from Fig. 5-6 that for the same charging power the PCM store temperature T_{mean} is higher than the temperature T_{upper}. In the start of the charging process, the difference between T_{mean} and T_{upper} reaches up to 30K. The difference decreases gradually with melting of the PCM material. When the store temperature is in the range of 50-60ºC, the difference between T_{mean} and T_{upper} becomes insignificant. The charging power decreases gradually with increase of the PCM store temperature. With an increase of the charging volume flow rate, the charging power at the later stage of the charging process increases.

The CFD predicted power versus temperature of the PCM store is shown as circles in Fig. 5 and 6. For the same temperature of the store, the CFD predicted power of a solid phase PCM module is higher than the power determined based on T_{upper} while it is lower than the power determined based on T_{mean}.

The CFD predicted power of liquid phase PCM is higher than the measured power. The viscosity of the liquid phase PCM could be underestimated by equation 4 in the CFD calculations, resulting in an overestimated convective heat transfer and a higher charging power. The disagreement could be caused by errors in the experiments. However these theories need to be confirmed in future investigations.

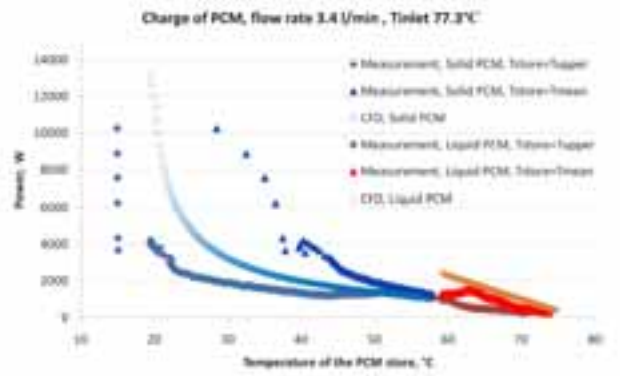

Fig. 5: Charging power vs. temperature of the PCM store for a volume flow rate of 3.4 l/min.

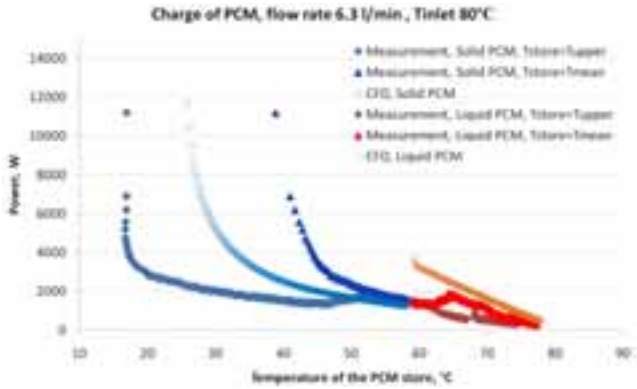

Fig. 6: Charging power vs. temperature of the PCM store for a volume flow rate of 6.3 l/min.

Heat exchange capacity rate of the PCM module is determined using equation (10). Fig. 7 and 8 show heat exchange capacity rate versus temperature of the PCM store for volume flow rates of 3.4 l/min and 6.3 l/min respectively. The heat exchange capacity rate of solid phase PCM lies in the range of 40-450 W/K. In the very start of the test, the heat exchange capacity rate is within 150-450 W/K due to large thermal capacity of the PCM module and replacement of the cold water in the heat exchange by inlet hot water. The heat exchange capacity rate determined based on T_{mean} decreases from 150 W/K to 75 W/K with increase of the PCM store temperature from 40ºC to 58ºC while the heat exchange capacity rate determined based on T_{upper} firstly decreases to 40 W/K and keeps almost constant until the temperature of the PCM store reaches 45-48ºC. The heat exchange capacity rates determined based on the two PCM store temperatures tend to be the same for a store temperature close to 58ºC. The CFD predicted heat exchange capacity rate of solid PCM is higher than the heat exchange capacity rate determined by T_{upper} and lower than that determined by T_{mean}. The difference between the CFD calculated and the measured capacity rate can be explained by the incorrect representation of store temperature of either T_{upper} or T_{mean}.

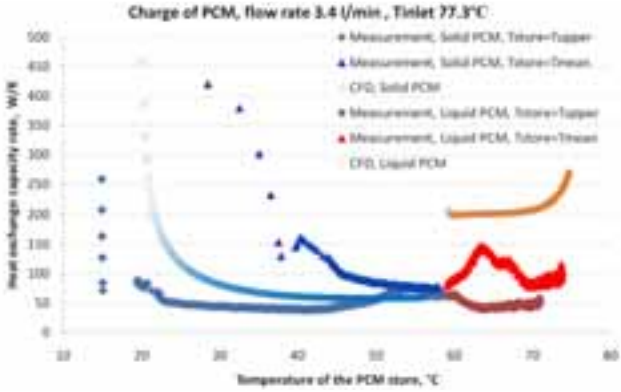

Fig. 7: Heat exchange capacity rate vs. temperature of the PCM store for a volume flow rate of 3.4 l/min.

The heat exchange capacity rate of a liquid phase PCM store determined based on T_{mean} is in the range of 75 W/K-150 W/K while it is in the range of 40-80 W/K if T_{upper} is used to plot heat exchange capacity rate. When the store temperature is higher than 58ºC, the PCM in the store should be in a liquid phase which

should give a higher convective heat transfer rate, however the measurements show that the heat exchange capacity rate of a liquid phase PCM determined based on T_{mean} is only slightly higher than the capacity rate of a solid phase PCM. The heat exchange capacity rate determined based on T_{upper} decreases slightly. There is a need for further investigations to detect the reasons. The CFD predicted heat exchange capacity rate of liquid PCM is higher than the measured capacity rates.

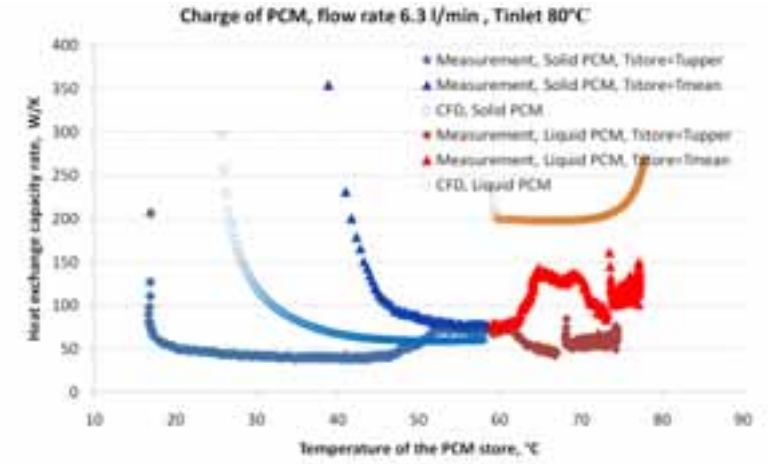

Fig. 8: Heat exchange capacity rate vs. temperature of the PCM store for a volume flow rate of 6.3 l/min.

The measured heat exchange capacity rates of a solid PCM for different charging volume flow rates are summarized in Fig. 9. It is shown that the charging volume flow rate has an insignificant influence on the heat exchange capacity rate of a solid phase PCM store. This implies that the heat transfer in the heat exchanger is not critical and thus have a minor influence on the heat exchange capacity rate between water and the PCM store.

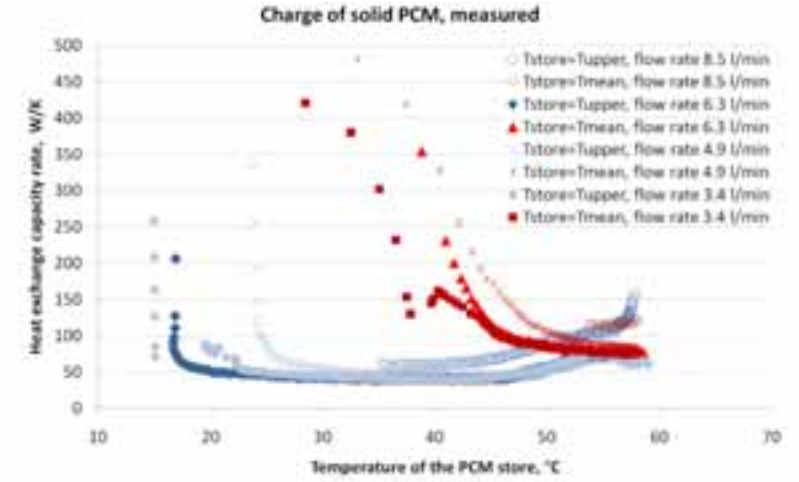

Fig. 9: Measured heat exchange capacity rate vs. temperature of the PCM store for different volume flow rates.

The CFD predicted heat exchange capacity rates for different charging volume flow rates are shown in Fig. 10. It is shown that the heat exchange capacity rate of a liquid PCM is around 200-250 W/K which is more than 3 times higher than the heat exchange capacity rate of a solid PCM if the store temperature is higher than 40ºC. As shown in Fig. 7 and 8, the measured heat exchange capacity rate of liquid phase PCM is within 40-150 W/K. The disagreement between the CFD calculation and the experiments could be explained by the viscosity of the liquid phase PCM which is much higher than anticipated in the CFD calculations.

4.2 Charge of a supercooled liquid PCM

The charge behaviour of a supercooled liquid PCM is investigated. The charge test starts with a uniform temperature of 16-18ºC and with a constant inlet temperature of 77-80ºC. Fig. 11 and 12 show the charging power of a supercooled liquid PCM heated with volume flow rates of 3.1 l/min and 7.1 l/min respectively. The charging power is higher than 4000 W when the store temperature T_{upper} is lower than 45ºC or the store temperature T_{mean} is lower than 58 ºC. Compared with charge of a solid phase PCM, the charging power of a

supercooled liquid is higher than the charging power of a solid PCM at the same store temperature. The CFD predicted charging power shows similar trend.

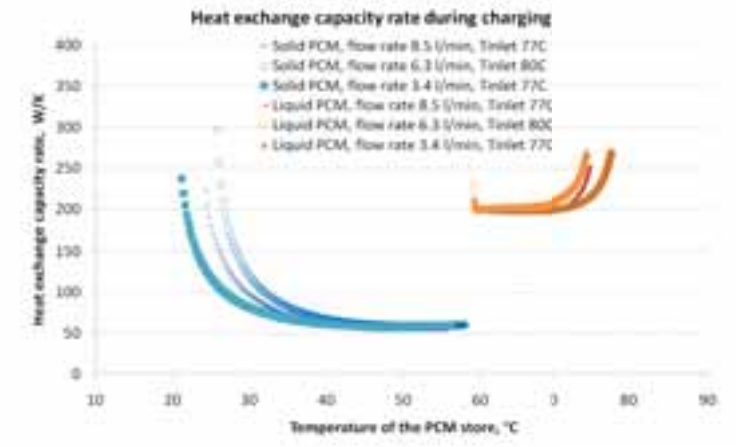

Fig. 10: CFD predicted heat exchange capacity rate vs. temperature of the PCM store for different volume flow rates.

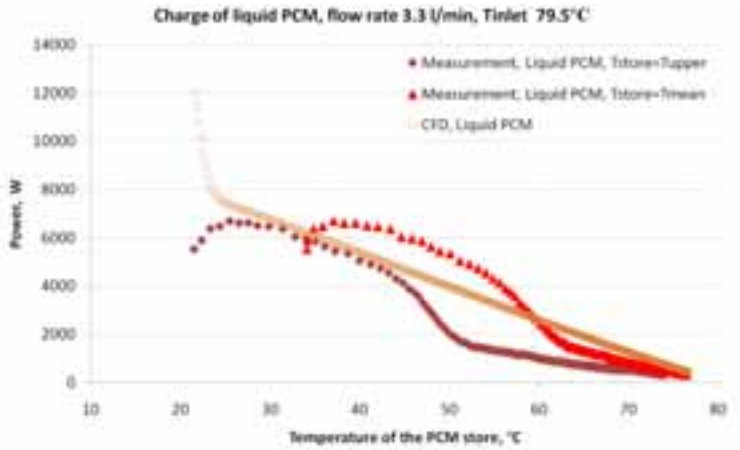

Fig. 11: Charging power vs. temperature of the PCM store for a supercooled PCM with a charging flow rate of 3.3 l/min.

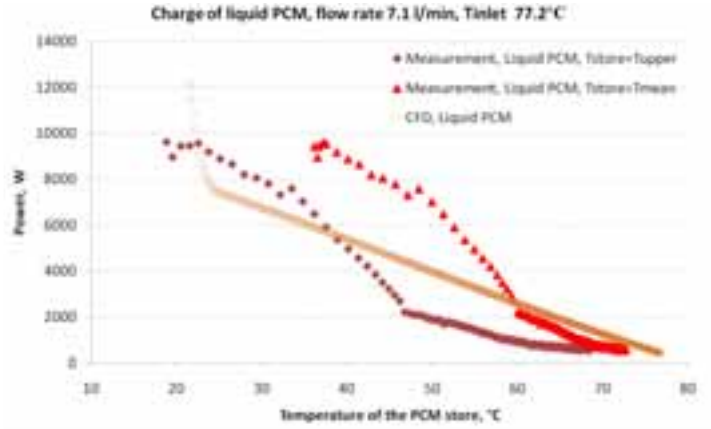

Fig. 12: Charging power vs. temperature of the PCM store for a supercooled PCM with a charging flow rate of 7.1 l/min.

The heat exchange capacity rate of a supercooled liquid PCM is show in Fig. 13 and 14. Fig. 13 show the heat exchange capacity rate versus temperature of the PCM store heated with a volume flow rate of 3.3 l/min. The heat exchange capacity rate determined based on T_{upper} reaches up to 200 W/K when the store temperature T_{upper} is within 30-40ºC. The capacity rate drops to approx. 50 W/K if the temperature of the store T_{upper} is higher than 50ºC. The heat exchange capacity rate determined based on T_{mean} is higher than the heat exchange capacity rate determined based on T_{upper}. The CFD predicted heat exchange capacity rate is in the range of 200-250W/K. Possible explanation of the disagreement could be the molecular structure change of SAT when supercooled. Even though there is no apparent crystallization, the molecular structure of SAT has been changed, which results in a PCM in between liquid phase and gel. Observation shows that fibre like

structures grow in the bottom part of the liquid when supercooled, forming a gel like liquid with a dramatically increased viscosity. When charged, the fibre structure will absorb heat and undergo molecular structural changes. The influence of the fibre structures on fluid flow and heat transfer in the PCM store can not be considered in the CFD models.

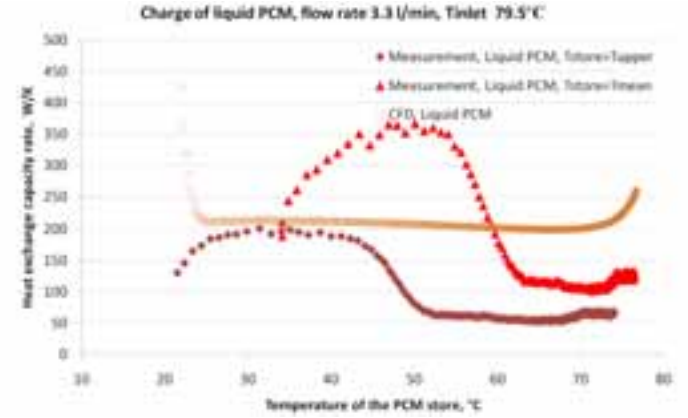

Fig. 13: Heat exchange capacity rate for a supercooled PCM with a charging flow rate of 3.3 l/min.

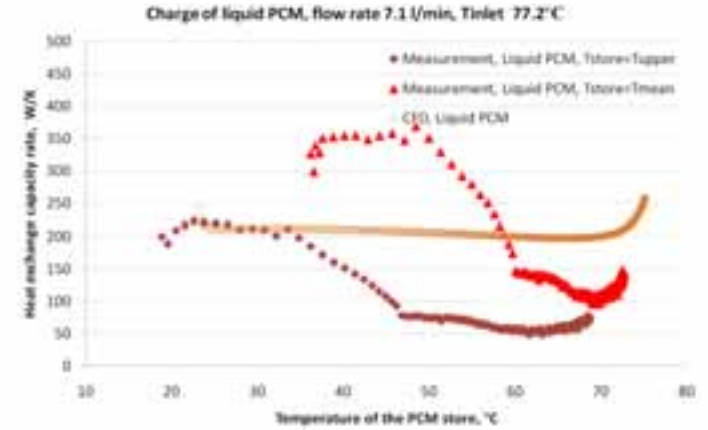

Fig. 14: Heat exchange capacity rate for a supercooled PCM with a charging flow rate of 7.1 l/min.

4.2 Discharging of the PCM module

Discharging of the liquid PCM is investigated with volume flow rates of 3.3 l/min, 4.2 l/min and 7.1 l/min. The discharge test starts with a uniform temperature of about 77-80ºC and with a constant inlet temperature of about 14-16ºC. Fig. 15 shows discharging power versus temperature of the PCM store where liquid PCM is crystallized during the discharge, while Fig. 16 shows discharging power of a liquid PCM where crystallization does not happen. With decrease of the store temperature, there is decrease of discharging power. The difference between the store temperature T_{bottom} and T_{mean} is larger with a crystallization of PCM than the temperature difference without crystallization. It is shown in Fig. 16 that even though crystallization does not occur, the inclination of the curve of the discharge power drops when the bottom surface temperature is lower than 58ºC. Such a change of inclination of the discharging power of a liquid PCM is not shown in Fig. 15, indicating changing of the PCM properties when PCM is supercooled.

Fig. 17 and 18 show the heat exchange capacity rate during discharging of the PCM module. Fig. 17 shows the heat exchange capacity rate of liquid phase PCM and crystallized PCM while Fig. 18 shows the heat exchange capacity rate of a liquid phase PCM without crystallization. The heat exchange capacity rate of a liquid phase PCM is around 250 W/K at the start of the discharging. As the temperature of the store decreases, the heat exchange capacity rate decreases to around 50 W/K as temperature of the store drops to 20-30ºC. The CFD model predicts satisfactorily the heat exchange capacity rate of a solid phase PCM but there is a significant disagreement in prediction of a liquid phase PCM.

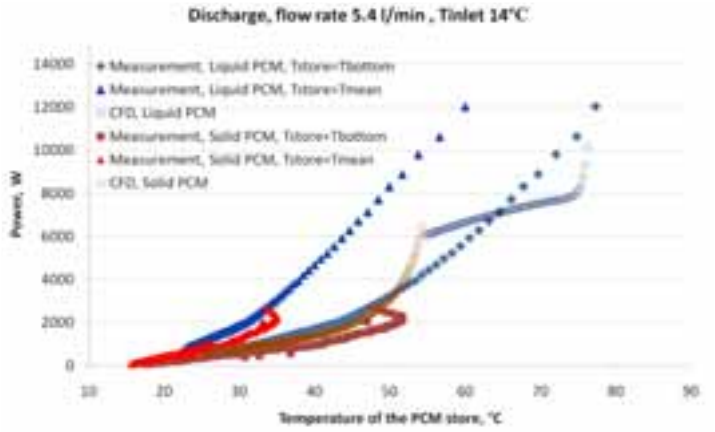

Fig. 15: Discharging power of a liquid PCM with a discharging flow rate of 5.4 l/min.

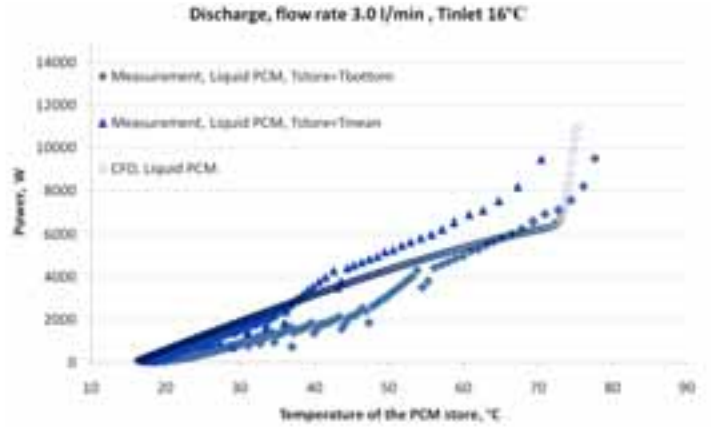

Fig. 16: Discharging power of a liquid PCM with a discharging flow rate of 3.0 l/min.

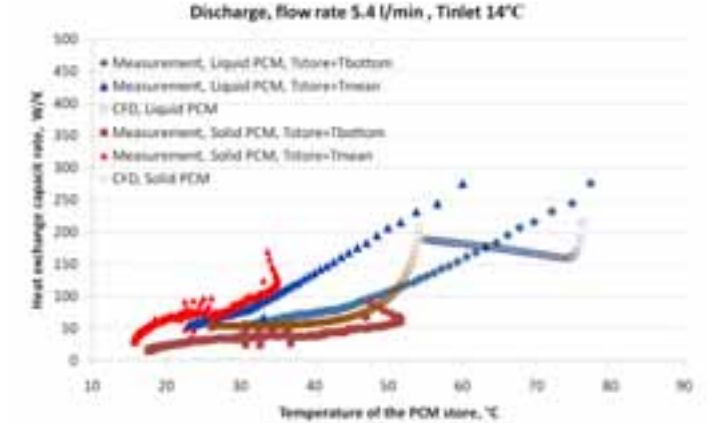

Fig. 17: Heat exchange capacity rate of a liquid PCM with a discharging flow rate of 5.4 l/min.

5. Conclusions

Thermal experiments and CFD simulations have been carried out to investigate the heat exchange capacity from and to the PCM module. The heat transfer rate between the PCM box and the heating fluid/cooling fluid in the plate heat exchangers is determined. Table 1, 2 and 3 list respectively the power weighted average of heat exchange capacity rate during charge of the PCM module, during charge of supercooled PCM and during discharge of the PCM module. The measured heat exchange capacity rate during charge of a solid phase PCM is within 67-170 W/K. For charge of liquid PCM, the measured heat exchange capacity rate is 50-112 W/K while it is 134-265 W/K for charge of supercooled liquid PCM. The CFD predicted capacity rate for charge of solid PCM and liquid PCM is 90-95 W/K and 199-213 W/K respectively.

For discharge of the PCM module, the measured heat exchange capacity rate of liquid PCM is 127-242 W/K while it is 48-94 W/K for solid PCM. The CFD predicted heat exchange capacity rate during discharge of liquid PCM and during discharge of solid PCM is 171-400 W/K and 50-350 W/K respectively.

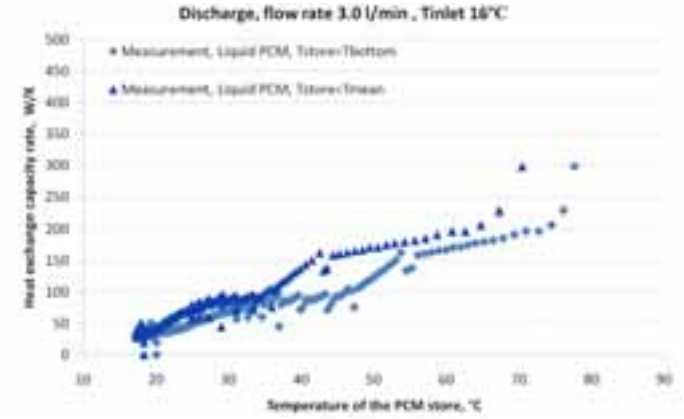

Fig. 18: Heat exchange capacity rate of a liquid PCM with a discharging flow rate of 5.4 l/min.

It can be concluded that the CFD model of solid phase PCM predicts satisfactorily the heat exchange capacity rate between the PCM module and water while there is a significant disagreement between the CFD predicted and the measured capacity rate of liquid PCM module. Possible explanation could be the change of molecular structure of liquid SAT resulting in huge variations in the viscosity during charge and discharge which can not be considered in the CFD model. A multi-phase CFD model would be recommended in the future to determine the cause of the disagreement. The measured heat exchange capacity rates are about a factor of 1.5-5 of the desired value 250 W/K, both for charge and discharge periods. It is expected that if the heat is transferred both by means of water flowing through the upper and the lower room, the heat exchange capacity rates will still be a factor of 1-2.5 too low for charge periods and for discharge periods. Based on the investigations, a new 300 l flat heat storage module with increased heat transfer areas was constructed (Furbo etc., 2011). Further thermal measurement on the new storage module will be used to validate the CFD models. It is expected that the new heat storage module will have good thermal characteristics inclusive sufficiently high heat exchange capacity rates.

Table 1. Power weighted average of heat exchange capacity rate during charge of the PCM module.

Volume flow rate		Measured heat exchange capacity rate		CFD predicted heat exchange capacity rate	
		Solid phase	Liquid phase	Solid phase	Liquid phase
		W/K	W/K	W/K	W/K
		T_{store}=17-58ºC	T_{store}=58-80ºC	T_{store}=17-58ºC	T_{store}=58-80ºC
3.4 l/min	Tstore=Tupper	71	50	90	205
	Tstore=Tmean	143	107		
4.9 l/min	Tstore=Tupper	67	57	90	200
	Tstore=Tmean	141	112		
6.3 l/min	Tstore=Tupper	81	58	95	199
	Tstore=Tmean	170	112		

Table 2. Power weighted average of heat exchange capacity rate during charge of supercooled PCM module.

Volume flow rate		Measured heat exchange capacity rate		CFD predicted heat exchange capacity rate	
		Solid phase	Liquid phase	Solid phase	Liquid phase
		W/K	W/K	W/K	W/K
		-	T_{store}=16-80ºC	-	T_{store}=16-80ºC
3.1 l/min	Tstore=Tupper	-	134	-	211
	Tstore=Tmean	-	222		
4.1 l/min	Tstore=Tupper	-	158	-	210
	Tstore=Tmean	-	256		
7.1 l/min	Tstore=Tupper	-	158	-	213
	Tstore=Tmean	-	265		

Table 3. Power weighted average of heat exchange capacity rate during discharge of the PCM module.

Volume flow rate		Measured heat exchange capacity rate		CFD predicted heat exchange capacity rate	
		Solid phase	Liquid phase	Solid phase	Liquid phase
		W/K	W/K	W/K	W/K
		T_{store}=14-58ºC	T_{store}=58-80ºC	T_{store}=14-58ºC	T_{store}=58-80ºC
5.4 l/min	Tstore=Tupper	48	127	89	205
	Tstore=Tmean	94	242		
3.0 l/min		-	T_{store}=14-80ºC		T_{store}=14-80ºC
No cyrstallization	Tstore=Tupper	-	143	-	202
	Tstore=Tmean	-	241		

6. Nomenclature

C_p Specific heat, [J/(Kg.K)]
H Heat exchange capacity rate, [W/K]
P Charging/discharging power, [W]
T Temperature, [K].
V Volume flow rate of the charging/discharging flow, [m^3/s]
λ Thermal conductivity, [W/(mK)]
ρ Density, [kg/m^3]
μ Dynamic viscosity, [kg/(ms)]
Subscript
f, r, s inlet (forward), outlet (return) and store respectively.

7. References

Furbo, S., Dragsted, J., Chen, Z., Fan, J., Andersen, E., Perers, B., 2010. Towards seasonal heat storage based on stable supercooling of sodium acetate trihydrate. EuroSun 2010 Congress Proceedings, Graz, Austria.

Furbo, S., 1978. Investigations of heat storages with salt hydrate as storage medium based on the extra water principle. Thermal Insulation Laboratory, Technical University of Denmark, report no. 80.

Schultz, J.M., Furbo, S., 2007. Solar heating systems with heat of fusion storage with 100% solar fraction for low energy buildings. ISES Solar World 2007 Congress proceedings. Beijing, China.

Ansys Inc., 2010. “Ansys Fluent release 13.0”, Southpointe, 275 Technology Drive, Canonsburg, PA 15317, U.S.A.

Ariki N., Futamura M., Makino A., Shibata H., 1995. Measurement of thermophysical properties of sodium acetate hydrate. International Journal of Thermophysics, 16(6) pp. 1455-1466.

Yoon W., Shul Y., Kim J., etc. 2000. Encapsulation of sodium acetate trihydrate and stearic acid for thermal energy storage. Journal of the Korean Institute of Chemical Engineering, 38(5) pp. 725-731.

Furbo, S., Dragsted, J., Fan, J., Chen, Z., Andersen, E., Perers, B., 2011. Experimental studies on seasonal heat storage based on stable supercooling of a sodium acetate water mixture. ISES Solar World Congress 2011 Proceedings, Kassel, Germany.